

SLAC TRANS – 0212

TRANSLATION

TITLE : — as translated into,
ENGLISH FROM GERMAN

DESIGN, FUNCTION AND EFFECT
OF ERRORS OF LINEAR LASER
INTERFEROMETERS

AUTHOR(S) : Andreas Welz

SOURCE : Source not Indicated

Translated: May 1984

for: SLAC, Stanford, CA

by: AD-EX Translations International/USA

Seminar Paper

by

cand. geod. mont. Andreas Welz

Subject:

Design, function and effect of errors
of linear laser interferometers

Contents

	<u>Page</u>
1. Introduction	3
2. Physical principles	4
2.1 Interference	4
2.2 Coherence	6
2.3 Doppler effect	10
3. The Michelson interferometer	11
3.1 Mode of operation	11
3.2 Systematic errors of the Michelson interferometer	21
3.2.1 Effect of errors due to the laser	21
3.2.2 Influence of refraction	27
3.3 Accuracy and resolution	33
4. The laser Doppler interferometer	37
4.1 Mode of operation	37
4.2 Systematic errors of the laser Doppler interferometer	41
4.2.1 Effect of errors due to the laser	41
4.2.2 Influence of refraction	42
4.3 Accuracy and resolution	43

Appendix

Literature

1. Introduction

Because of the technological progress in recent decades, the conventional tools for length measurement, such as meter sticks, tape measures, micrometer screws or travelling microscopes, can no longer adequately meet the requirements of accuracy, speed and automation.

The machine fabrication industry needs measuring tools with a measurement accuracy of 0.5 to 1.5 microns per meter for checking the straightness, flatness, squareness, parallelism and circular runout of finished machine parts.

Geodesy requires a tool for measuring length with a relative accuracy of one part per million in order to calibrate its precision measuring instruments, such as the invar-ribbon level rod, the standard meter or the stadia rod.

In the manufacture of optical glasses, the thickness of evaporated coatings (around 0.13 microns) must be measured and adjusted exactly to the required value.

The interferometer is an instrument which can meet these requirements. Interferometry was actually used for the first time almost 100 years ago, but because of experimental problems with the available light sources was virtually abandoned. Only the advent of the laser led to increased use of interferometers. The laser interferometers now on the market are capable of measuring lengths up to 60 m with a resolution of 0.1 to 0.01 microns.

2. Physical principles

2.1. Interference

Interference is the intensification or attenuation of waves by superposition of two or more waves propagating in the same direction. Interference phenomena are only observable, however, if a coherent light source is used. In other words, the emitted light waves have a constant phase difference over a given time period. The concept of coherence is explained in more detail in Section 2.2. Interference occurs in two ways:

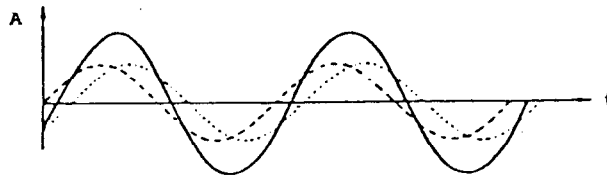


Figure 1

Figure 1 shows the interference of two waves with identical frequency and constant phase difference p . The resultant wave can be determined by the principle of superposition. The frequency of the resultant wave is equal to that of the initial waves, but the phase and amplitude have changed.

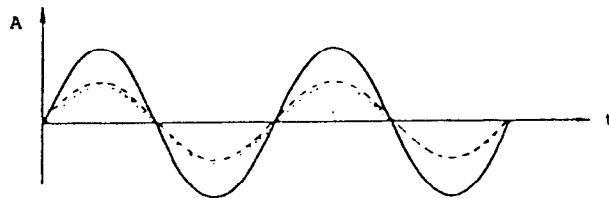


Figure 2

Figure 2 illustrates the special case in which the phase difference p is equal to zero. If the interfering waves have equal amplitudes, the resultant wave has double the amplitude of the individual waves. The frequency of the resultant wave is again equal to that of the original waves.

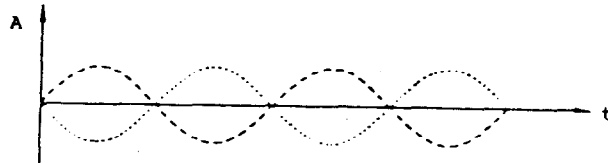


Figure 3

If the phase difference is equal to π and the amplitudes of the interfering waves are identical, the wave will be annulled (Figure 3).

Another form of interference occurs between two waves of different frequencies. However, the frequency difference must be very small. Figure 4 illustrates the interference between two waves under these conditions.

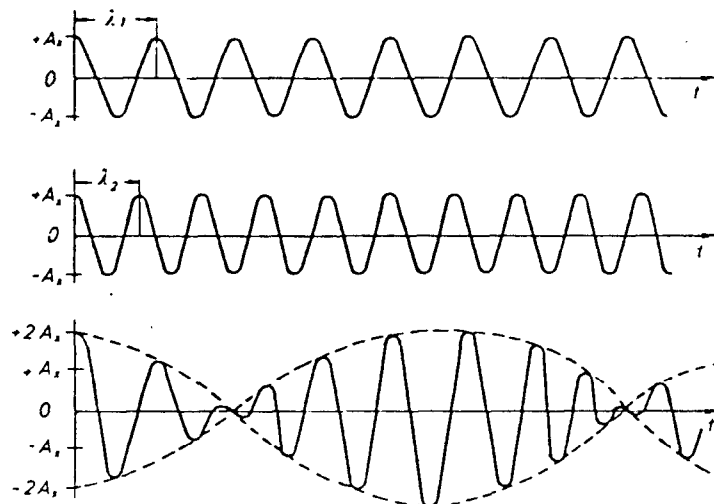


Figure 4: Interference of two waves of similar frequencies f_1 and f_2

The resultant wave can again be determined by superposition of the two original waves. Beating occurs with a frequency corresponding to the frequency difference $f_1 - f_2$. The beat wavelength is obtained from the formula:

$$\lambda_{\text{beat}} = \frac{c}{f_1 - f_2}$$

where c = velocity of light,

f = frequency of the waves,

and so

$$\lambda_{\text{beat}} = \frac{\lambda_1 \cdot \lambda_2}{\lambda_1 - \lambda_2} \approx \frac{\lambda_1^2}{\Delta\lambda}$$

2.2. Coherence

A distinction is made between time coherence and space coherence. Time coherence of two waves exists if the phase difference remains constant during a given time period. This definition implies that time-coherent waves must have the same frequency and that their path difference is constant over a fixed time period. Space coherence refers to the maximum spatial extent over which the phase relationship between the two waves remains constant.

Wave trains with no fixed relationship to each other in space and time are known as incoherent wave trains. However, coherence is not an absolute quantity, since there are

different degrees of coherence, for the reason that exactly periodic waves practically do not exist. Each frequency can vary within a bandwidth Δf .

This bandwidth Δf depends on the frequency f .

The frequency variation within the bandwidth leads to a time limitation for coherence. The coherence time is defined as the reciprocal of the bandwidth.

$$t_{\text{coherence}} = \frac{1}{\Delta f}$$

where f is expressed in Hz.

This represents the minimum time period within which the phase and frequency of a wave do not vary. From the coherence time and the wave propagation velocity (equal to c in air) it is possible to calculate the coherence length, which represents the distance over which the wave can be coherent with other waves.

$$l_{\text{coherence}} = c \cdot t_{\text{coherence}} = \frac{c}{\Delta f}$$

Table 1

	Bandwidth Hz	Coherence time sec	Coherence length m
Visible spectrum	2×10^{14}	5×10^{-15}	10^{-6}
Monochromatic light	10^9	10^{-9}	3×10^{-1}
HeNe gas laser	3 to 10^4	0.3 to 10^{-4}	3×10^4 to 10^8

Comparison of the coherence of some radiation sources reveals distinct differences. Visible light has a large bandwidth and a very short coherence length. To understand this it is necessary to know how visible light is produced. In conventional light sources such as the sun, incandescent bulbs and fluorescent lights, atoms are excited from their ground state by absorption of thermal or electrical energy. In other words, electrons bound to an atom absorb a quantum of energy and, as a result, leave their shell and enter a higher energy level.

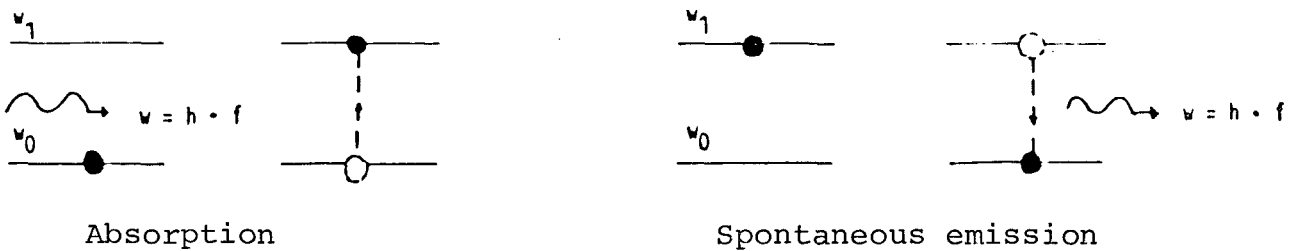


Figure 5

After a short lifetime, usually on the order of 10^{-8} sec, they return to the ground state by emitting the absorbed energy in the form of a light quantum (photon). This process is known as "spontaneous" emission. Since the energy of the emitted photons is not constant, but depends on the energy level from which the electron returns to its ground state, the frequency or wavelength of the emitted light is not constant. Also, since the atoms radiate at different instants, the path difference between the wave trains varies continuously.

Consequently, the phase relationship between the wave trains varies randomly in time. This situation is responsible for the small coherence length of the light. Thus visible light is known as incoherent, and is not suitable for interferometry.

The time coherence of visible light can be improved if the emitted light rays are sent through a filter which passes only a single wave or a narrow wavelength range. Space coherence can be improved by placing a slit in the radiation path. Monochromatic light with a coherence length of 0.3 to 1.0 m is obtained. However, the light intensity is greatly reduced by the filter and slit, and thus is inadequate for most measurements.

As Table 1 shows, the light emitted by the HeNe laser is confined within a narrow bandwidth, thus leading to a large coherence length for that light. Such light is produced by stimulated emission of photons. In stimulated emission, an energy quantum impinges on an excited atom and causes it to emit another similar quantum before it has time for spontaneous emission.

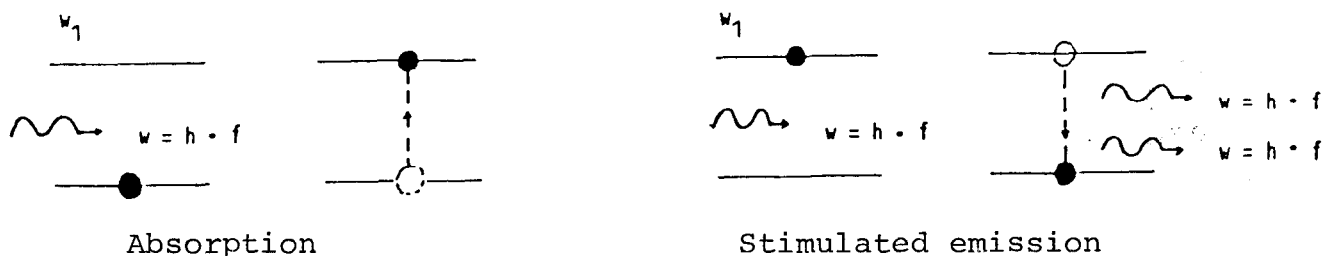


Figure 6

Stimulated emission is possible only if inversion exists, i.e., more atoms must be present in the excited state than in the ground state. The stimulated electromagnetic wave has the same frequency, phase, propagation direction and vibration planes as the inducing radiation. Thus the stimulated wave satisfies the coherence conditions and is therefore suitable for interferometry. Moreover, the emitted radiation is extremely intense and can be tracked for several kilometers.

It is quite apparent that the interferometer became a usable measuring instrument only by virtue of the development of the laser.

2.3. Doppler effect

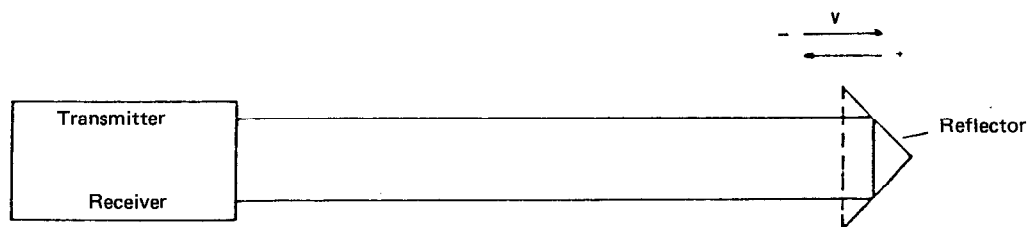


Figure 7

If the reflector is moved with velocity V , the frequency f_s of the transmitted beam is changed by the Doppler frequency f_d . At the reflector, the emitted wave has the following frequency:

$$f_R = f_s \left(1 \pm \frac{v}{c} \right) \quad \text{Doppler component}$$

Since the motion of the reflector acts twice on the receiver frequency (the reflector is moving along both the forward and return paths of the wave), the receiver frequency f_E is given by:

$$f_E = f_s \left(1 \pm \frac{2v}{c} \right)$$

The Doppler component f_D is calculated from $f_D = f_E - f_s$.

Thus

$$f_D = f_s \pm f_s \cdot \frac{2v}{c} - f_s$$

$$f_D = \pm f_s \cdot \frac{2v}{c} \quad \text{mit } f_s = \frac{c}{\lambda}$$

$$\underset{\text{=====}}{f_D = \frac{2v}{\lambda}} \implies \underset{\text{=====}}{v = f_D \cdot \frac{\lambda}{2}}$$

The sign of the Doppler frequency depends on the direction of motion of the reflector. It is positive for motion towards the interferometer and negative for motion in the opposite direction.

3. The Michelson interferometer

3.1. Mode of operation

The Michelson interferometer is one of the oldest interferometers, and as early as 1882 was used successfully to define the length

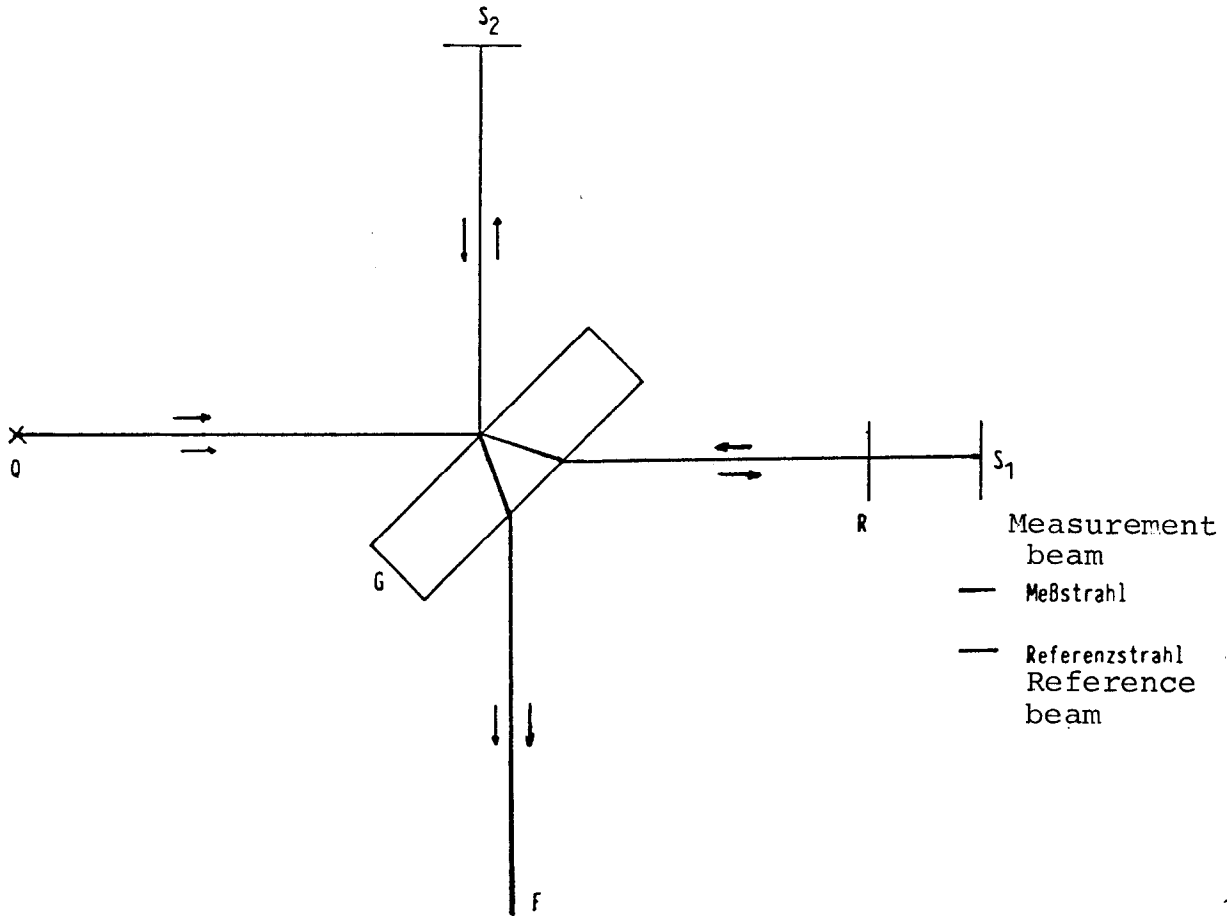


Figure 8

of the standard meter in numbers of wavelengths of the red line of cadmium. It is named for the physicist A. A. Michelson, its inventor. The classical layout of the Michelson interferometer is illustrated in Figure 8.

G is a half-silvered plane-parallel glass plate tilted at 45° to the light beam Q . S_1 and S_2 are two plane mirrors, which are placed as closely as possible at right angles to each other. Light from source Q falls on the front side of the glass plate,

which is coated with a semitransparent reflective metal film. The light is thus split into a reference beam RS and a measurement beam MS. Reference beam RS passes through the glass plate and falls on mirror S_2 from which it is reflected back to G. Here it is again split into two partial beams, one of which returns to the light source and is of no further interest, while the other is reflected into an observation telescope F. Measurement beam MS is reflected from the glass plate towards mirror S_1 . Part of the light reflected at S_1 is reflected at the reflective coating and ignored. The rest passes through the glass plate and also arrives in observation telescope F. In viewing from the source Q towards the reflective coating of the glass plate, the virtual image of mirror S_2 can be seen at R, the reference plane. Thus the reflection at S_2 can be replaced conceptually by a reflection at reference plane R. If S_1 and S_2 are almost perpendicular to each other and the glass plate is tilted at 45° to the light beam, S_1 and R will be almost parallel. This case is comparable to interference in an air wedge.

The situation is illustrated once more in Figure 9. The reference and measurement beams are subjected to an optical phase shift of $\lambda/2$ because of reflection at a denser medium. The measurement beam travels the additional geometric distance $2d$. By definition of the optical path length, this corresponds to the product of geometric distance and refractive

* Translator's note: This description is not consistent with Figure 8, but is almost a word-for-word translation of the German.

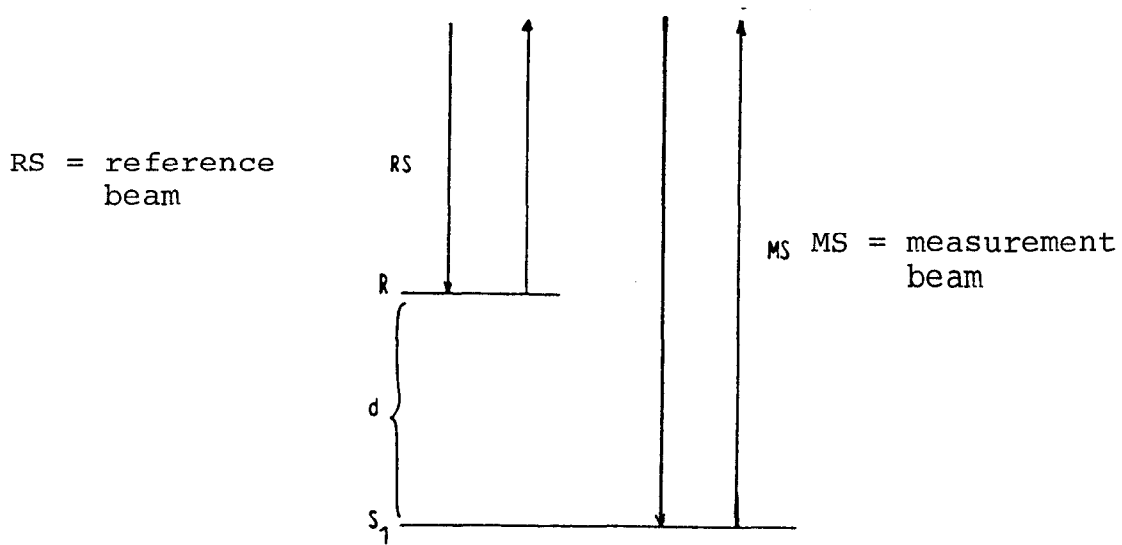


Figure 9

index of the medium being traversed: $S_{op} = 2 \cdot d \cdot n$. A further optical path shift of $\lambda/2$ occurs due to reflection of the measurement beam at the glass plate. This means that both beams have now been subjected to an optical path shift of $\lambda/2$ by reflection at the mirror, and so the two shifts cancel each other out to zero. The remaining differences are the optical path difference of the measurement beam in the air wedge and the path shift due to reflection of the measurement beam at the glass plate. If the reference beam and measurement beam are to interfere constructively, the following condition must be satisfied:

$$S_{op} = K \cdot \lambda \quad \text{with } K = 1, 2, 3, 4 \dots \text{ (corresponds to phase shift} = 0)$$

$$2 \cdot d \cdot n + \lambda/2 = K \cdot \lambda \quad n = 1 \text{ (air wedge)}$$

$$2d = K \cdot \lambda - \lambda/2$$

$$d = \frac{1}{2} K \cdot \lambda - \frac{1}{4} \lambda$$

$$d = \frac{2K - 1}{4} \cdot \lambda \quad \text{with } K = 1, 2, 3, 4$$

* Translator's note: Again, does not seem consistent with Figure 8 (number of reflections of measurement and reference beams).

Interference maxima are formed if the distance between S_1 and R (corresponding to thickness of the wedge) is equal to $1/4 \lambda$, $3/4 \lambda$, $5/4 \lambda \dots$. In general, one maximum follows another on changing the distance between S_1 and R by $\lambda/2$.

If the reference beam and measurement beam are to interfere destructively, the following condition must be satisfied:

$$S_{op} = K \cdot \lambda \quad \text{with } K = \frac{1}{2}, \frac{3}{2}, \frac{5}{2} \dots \quad (\text{corresponds to phase shift} = \pi)$$

$$d = \frac{2K - 1}{4} \cdot \lambda \quad \text{with } K = \frac{1}{2}, \frac{3}{2}, \frac{5}{2} \dots$$

Interference minima are formed if the distance between S_1 and R is equal to 0 , $\lambda/2$, λ , $3/2 \lambda \dots$. In general, once again, one minimum follows another on changing the distance by $\lambda/2$.

In the Michelson interferometer, the distance between S_1 and the reference plane is changed by moving mirror S_1 .

The interference patterns to be observed in the telescope then change. If S_1 and R are perfectly parallel, i.e., S_1 and S_2 are exactly perpendicular to each other, interference fringes of equal inclination (Haidinger's rings) are seen in F. When the distance between S_1 and R is increased or decreased by $\lambda/4$, bright and dark spots appear alternately at the center of the system of rings. In practice, rings spread out from the center if the distance is increased, and rings vanish at the center if the distance is decreased.

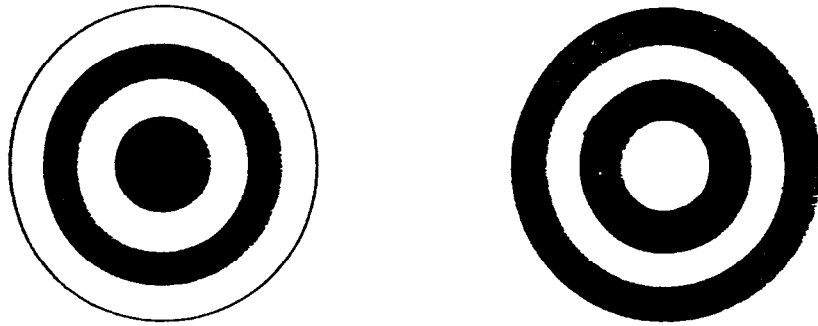


Figure 10: Change of the interference pattern when the distance between S_1 and R is changed by $\lambda/4$.

If S_1 and R are not perfectly parallel, a pattern of interference lines (Fizeau fringes) can be observed in the telescope. New fringes form at the center of the pattern if the distance between S_1 and R is increased, and fringes vanish at the center of the pattern if the distance is decreased.



Figure 11: Change of the interference pattern when the distance between S_1 and R is changed by $\lambda/4$.

A length can be measured by fixing its end points, moving mirror S_1 along the line between them and counting the resulting intensity maxima or minima. The number of maxima or minima counted is then multiplied by $\lambda/2$ to obtain the

measured length. The wavelength of the light thus becomes a measure of the optical path length travelled. For modern measurements, the classical layout of the Michelson interferometer has been greatly expanded.

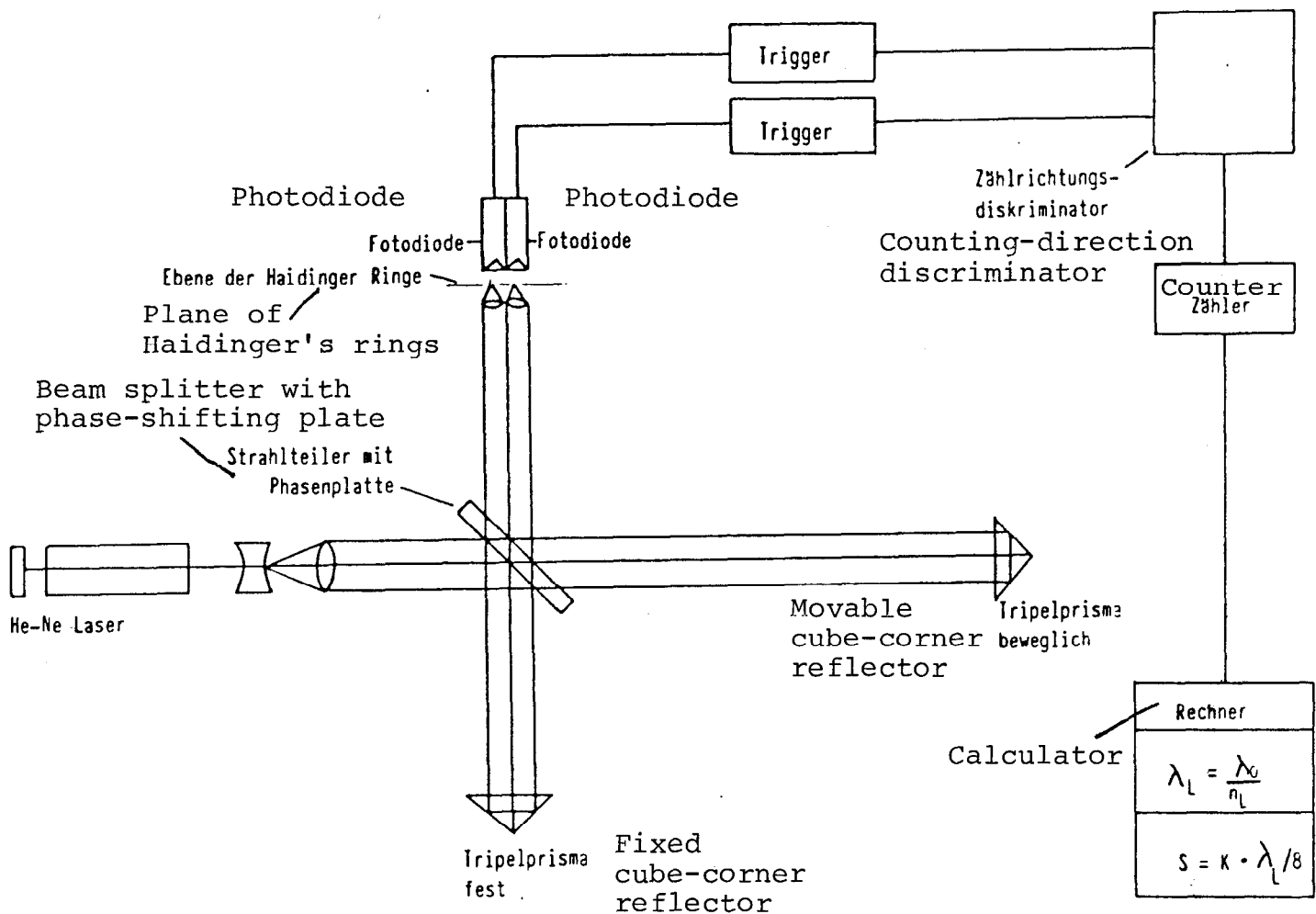


Figure 12

The monochromatic light source, which because of its small coherence length permitted only measurement of very short lengths, has been replaced by a frequency-stabilized laser. The plane-parallel mirrors, which are very expensive to manufacture, have been replaced by cube-corner reflectors, which do not have to be aligned with great precision. After reflection at all three mirror surfaces, incident light beams reemerge parallel to their angle of incidence, even if the beam direction and reflector axis are not parallel.

To improve the resolution, the glass plate has been replaced by a beam splitter with a quarter-wave phase-shifting plate. If the light emitted from the source is split into two partial beams, as can be achieved with a telescope, the beams reflected at the mirror surface have a path difference of $\lambda/4$. Consequently, the interference pattern produced on the screen

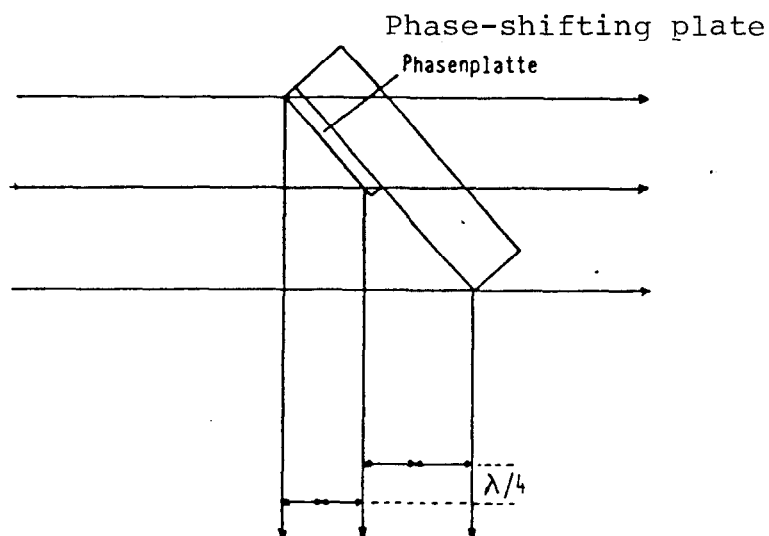
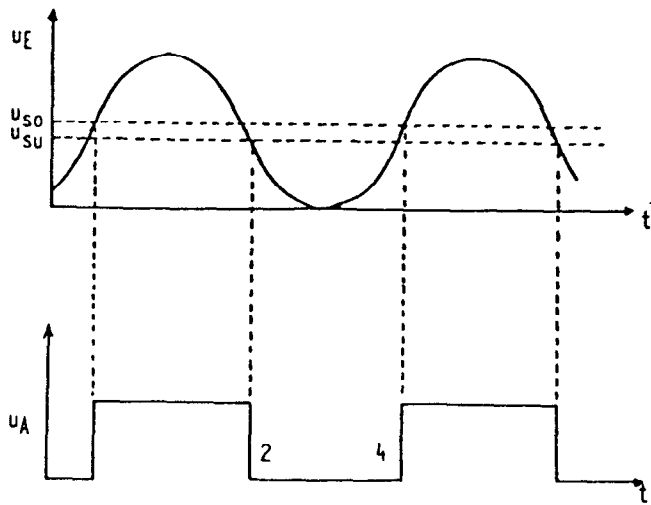


Figure 13

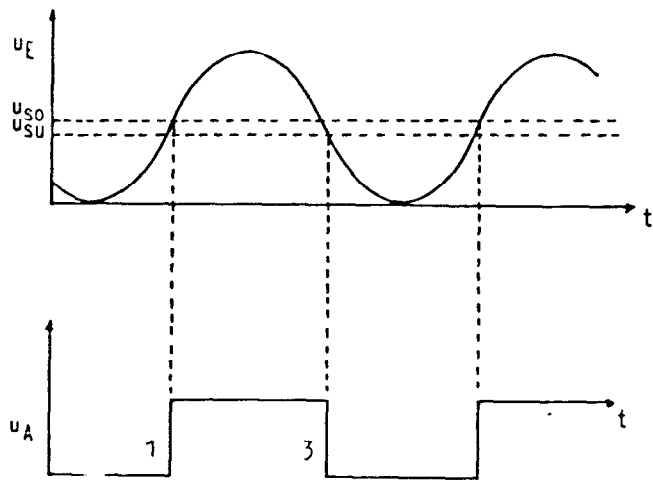
by the interfering waves are systems of Haidinger's rings with a quarter-wave phase shift. Holes through which the light is directed to photodiodes are positioned precisely in the region of the centers of the systems of rings. These photodiodes convert the intensity variations of the two centers to sinusoidal electrical signals. Two trigger levels transform the sinusoidal signals to square-wave signals. The input voltage to the trigger is proportional to the variations in intensity of the interferences at the center of the Haidinger's rings. As soon as the input voltage exceeds the upper threshold U_{so} , the output voltage changes from one binary signal to the other. It then changes back to the first binary signal only when the input voltage drops below the lower threshold U_{su} (Figure 14).

Each edge (1-4) of the two signals produces a counting pulse, and so four signals are formed per period. The path length can therefore be represented finely in basic units of $\lambda/8$ (approximately 0.08 microns). The counting direction is sensed with a counting-direction discriminator.



Fotodiode I
Photodiode I

Trigger I



Fotodiode II
(Verschiebung des Signals um $\lambda/4$)
Photodiode II
(Signal shifted by $\lambda/4$)

Trigger II

Figure 14

3.2. Systematic errors of the Michelson interferometer

3.2.1. Effect of errors due to the laser

As already explained, light with large coherence length and high long-time frequency stability is needed in interferometry. The frequency of the light emitted by a laser is a function of the resonator length. In simple lasers, thermal instability causes continuous variation of the resonator length and thus of the frequency of the emitted light. Thus simple lasers are not suitable for interferometric measurements.

The effects of a change in resonator length on frequency will be closely examined in the following. Accordingly, the frequency characteristics of laser light must first be discussed.

As already explained, light in a laser is produced by stimulated emission, in which a quantum of energy impinging on an excited atom causes it to emit another similar quantum. The atom then drops to a lower energy level. However, the energy $E = h \cdot f$ of the emitted quantum is not identical for each stimulated emission, but varies by small amounts ΔE . Consequently, the frequency of the stimulated electromagnetic wave also varies by small amounts Δf . This amount is known as the natural linewidth. In the case of gas lasers in particular, the natural linewidth is broadened by the Doppler effect, since the emitting atoms of the gas are moving relative to the direction of propagation of the light.

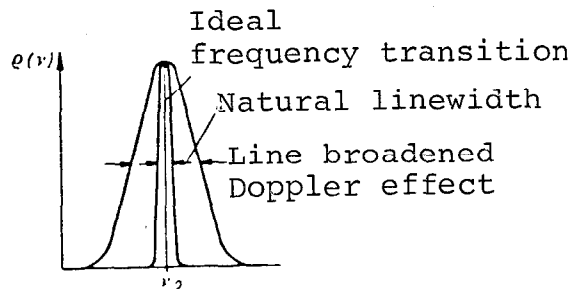


Figure 15: Natural linewidth and frequency transition broadened by Doppler effect.

Resonance must be established in order to amplify the electromagnetic wave. This occurs if the resonance condition $L = K \cdot \lambda/2$ (where λ = wavelength of the electromagnetic wave) is satisfied. Thus the resonator length must be a multiple of the half-wavelength. Since the resonator length is much larger than the wavelength of the emitted light, several resonance oscillations can be established simultaneously if the active medium has a large linewidth. Such oscillations are generally known as laser modes. They lie within the Doppler-broadened line and have themselves a certain linewidth. Both transverse and axial modes can occur. All modes which lie within the Doppler-broadened line and become amplified resonate in the emitted laser light and "contaminate" the frequency of the light. Transverse modes which are not desired can be filtered out by proper alignment of the resonator mirrors and by insertion of mode-selection diaphragms. However, it is much more difficult to select the axial modes. The interval between them depends on the resonator length, since:

$$\Delta f = \frac{c}{2L}$$

In principle, all but only those modes which lie within the amplification curve are amplified within the resonator. The amplification curve depends on the pumping energy supplied.

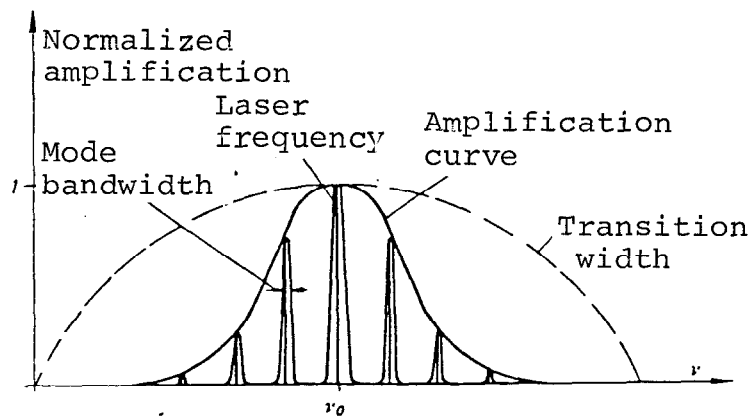


Figure 16: Linewidth of the laser transition, amplification in the resonator and laser frequency.

Figure 16 clearly shows that the frequency f_0 at the line center receives the greatest amplification in the resonator. The modes at intervals of Δf or $2\Delta f$ from the line center also resonate.

As the resonator length is decreased, the interval between the axial modes becomes larger. If the resonator length is decreased to the point that the axial interval between modes exceeds the half-linewidth, only f_0 is amplified. The laser is then known as a single-mode laser.

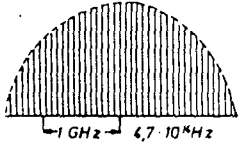




Output power mW	Resonator length m	Axial interval between modes MHz	
50	2	75	
25	1	150	
5	0.5	300	
1	0.2	750	
0.1	0.1	1500	

Figure 17: Interval between frequencies of the axial modes in TEM_{00} , and output power of the He-Ne laser for the wavelength of $\lambda = 632.8$ nm.

A numerical example for the He-Ne laser:

$$f_0 = 4.74 \times 10^{14} \text{ Hz} \implies \lambda_0 = \frac{c}{f_0}; \quad \lambda_0 = 0.6328 \text{ } \mu\text{m}$$

Resonance: $l = K \cdot \lambda/2$, with $K = 600,000$; $l = 0.190 \text{ m}$

Interval between modes $\Delta f = \frac{c}{2l} \approx 790 \text{ MHz}$

Ne linewidth: $\approx 1500 \text{ MHz} \implies$ single-mode laser

The light of the single-mode laser contains only the frequency $f_0 = 4.74 \times 10^{14} \text{ Hz}$.

However, if the length l of the resonator changes, the frequency of the single-mode laser also changes, since:

$$\frac{\Delta f}{f} = \frac{\Delta l}{l}$$

An example:

Change in resonator length, Δl : 10^{-6} m

Resonator length l : 0.190 m

Frequency of the laser light, f_0 : $4.7375158 \times 10^{14} \text{ Hz}$

$$\Delta f = \frac{\Delta l}{l} \cdot f_0 \approx 2496 \text{ MHz}$$

relative frequency error $\frac{\Delta f}{f} = 5 \times 10^{-6}$

Frequency of the laser light with changed resonator length

$$f_1: 4.7375407 \times 10^{14} \text{ Hz}$$

$$\lambda = \frac{c}{f} \quad \lambda_1 = 0.63279666 \text{ } \mu\text{m}$$

The length l of a measured distance is obtained by multiplying the total of all counted maxima or minima by $\lambda/2$. Let the number of counted maxima or minima be 1,000,000.

$$L_{\text{before}} = 1,000,000 \cdot \lambda_0/2 = 0.3164 \text{ m}$$

$$L_{\text{after}} = 1,000,000 \cdot \lambda_0/2 = 0.31639833 \text{ m}$$

The difference Δl between the two lengths determined before and after the change in resonator length is equal to

$$\underline{\underline{1.67 \times 10^{-6} \text{ m}}}$$

This error due to the change in resonator length greatly exceeds the resolving power of the interferometer (approximately 0.08 microns). Frequency-stabilization techniques have been developed in recent years to eliminate this source of errors. Depending on technique, the frequency is corrected by means of an adjustable resonator length or by decreasing the pumping power. The relative frequency error achieved depends on the particular technique, and lies between 600 parts per billion and 100 parts per trillion. For a resonator length of 0.190 m, these values correspond to a change Δl in resonator length on the order of 1.1×10^{-7} m to 1.9×10^{-11} m. The resulting frequency change lies between 284 and 0.05 MHz. This leads to errors ΔL in length measurement of 1.9×10^{-7} m to 1×10^{-11} m.

Obviously a relative frequency error of 600 parts per billion causes a length-measurement error Δl which already exceeds the resolving power of a good interferometer. Only frequency-stabilization techniques with relative frequency errors smaller than 1 part per billion permit sufficiently accurate length measurement. However, systematic length-measurement errors must also be expected. Rapid vibrations of the laser also cause changes in resonator length and thus frequency variations. Frequency-stabilization techniques compensate for such vibrations only with a time lag. Thus the laser station must be as free from vibrations as possible.

3.2.2. Influence of refraction

The wavelength of a light beam is constant in vacuum. In air, however, it is a function of air temperature and pressure and of the partial pressure of water vapor. These three variables, which describe the atmospheric conditions of the transmitting medium, are combined in the refractive index n . The actual wavelength is calculated from the formula:

$$\lambda_L = \frac{\lambda_0}{n}$$

In the following we examine how accurately each individual variable and thus the refractive index n must be determined in order to achieve a relative error of 100 parts per billion and less in length measurement.

The formula for reduction of electrooptically measured distances with unmodulated monochromatic light, developed in 1963 by BARREL and SEARS, can be applied without modification to laser interferometers.

The phase index n_{ph} of air is given by

$$n_{ph} = 1 + (287.604 + \frac{1.6288}{\lambda^2} + \frac{0.0136}{\lambda^4}) \cdot 10^{-6}$$

where λ is in microns.

This formula is valid for dry air at 0°C, an air pressure of 1013.3 mbar and a carbon dioxide concentration of 0.03%. Thus the phase index for an He-Ne laser with $\lambda = 0.6328$ microns is equal to 1.000291756.

Reduction to the actual refractive index n_L existing at the time of the measurement is based on the formula

$$n_L = 1 + \frac{n_{ph} - 1}{1 + \alpha \cdot T} \cdot \frac{p}{1013.3} - \frac{4.125 \cdot 10^{-8}}{1 + \alpha \cdot T} \cdot e$$

where T = dry-bulb temperature in °C,

e = partial pressure of water vapor in mbar,

α = 1/273.16°C,

p = air pressure in mbar.

According to SPRUNG and MAGNUS-TETENS*, the partial pressure of water vapor can be determined with the aspiration psychrometer from the equation

$$e = 10^{\left(\frac{7.5 \cdot T'}{T' + 237.3} + 0.6609\right) - 1/2 (T - T') \cdot \frac{p}{755}}$$

where T = dry-bulb temperature in °C,

T' = wet-bulb temperature in °C,

p = air pressure in bar.

The final formula for calculation of n_L is therefore:

$$n_L = 1 + \frac{(n_{ph} - 1)}{(1 + \alpha \cdot l) 1013.3} - \frac{4.125 \cdot 10^{-8}}{1 + \alpha \cdot l} \left(1.3 \cdot 10^{\left(\frac{7.5 \cdot T'}{T' + 237.3} + 0.6609\right) - 1/2 (T - T') \cdot \frac{p}{755}}\right)$$

To estimate the individual influences of the meteorological terms on n_L , it is necessary to differentiate the above equation with respect to T, p and T'. These differentiations are listed in the Appendix. The mean error of the refractive index n_L is then given as follows by the error propagation theorem:

$$m_{nL}^2 = \left(\frac{dn_L}{dT}\right)^2 \cdot m_T^2 + \left(\frac{dn_L}{dp}\right)^2 \cdot m_p^2 + \left(\frac{dn_L}{dT'}\right)^2 \cdot m_{T'}^2$$

* Translator's note: This name was hyphenated at the end of a line. The correct version could be MAGNUSTETENS, MAGNUS-TETENS or even MAGNUS and TETENS.

The individual influences of the meteorological terms on n_L are given by:

$$m_{nL}(T) = \frac{d_{nL}}{dT} \cdot m_T$$

$$m_{nL}(p) = \frac{d_{nL}}{dp} \cdot m_p$$

$$m_{nL}(T') = \frac{d_{nL}}{dT'} \cdot m_{T'}$$

For average atmospheric conditions ($T = 20^\circ\text{C}$, $T' = 15^\circ\text{C}$, $p = 960 \text{ mbar}$), numerical evaluation yields the following results:

$$m_{nL}(T) \sim - 8.52 \cdot 10^{-7} \cdot m_T \quad m_T \text{ in } ^\circ\text{C}$$

$$m_{nL}(p) \sim + 2.68 \cdot 10^{-7} \cdot m_p \quad m_p \text{ in mbar}$$

$$m_{nL}(T') \sim - 1.53 \cdot 10^{-6} \cdot m_{T'} \quad m_{T'} \text{ in } ^\circ\text{C}$$

If an accuracy of plus or minus 100 parts per billion is expected for n_L , i.e., $m_{nL} = \pm 1 \times 10^{-7}$, it is necessary to determine T , p and T' with the following accuracies:

$$m_T \sim \pm 0.12 \text{ } ^\circ\text{C} \quad m_p = 0 \quad m_{T'} = 0$$

$$m_p \sim \pm 0.37 \text{ bar} \quad m_T = 0 \quad m_{T'} = 0$$

$$m_{T'} \sim \pm 0.07 \text{ } ^\circ\text{C} \quad m_p = 0 \quad m_T = 0$$

These values show clearly that the measurements of temperature and air pressure must be undertaken very carefully in order to obtain highly accurate values of n_L .

Only then is high distance-measuring accuracy achieved, since:

$$L = K \cdot \frac{\lambda_0}{n_L \cdot 2}$$

Air turbulences in the region of the beam path cause changes in the refractive index of the air in that path and thus lead to changes in wavelength. Consequently, the number of waves corresponding to the measured distance is increased or decreased, leading to a change in the optical path length. A change in optical path length leads in turn to a change in the phase relationship between measurement and reference beams when they are combined in the interferometer, and thus influences the amplitudes of the interferences between the two waves. Under these conditions it is much more difficult to count the maxima; in particular, however, the working range of this measurement technique is reduced.

Vapor and dust in the region of the measurement beam also affect the Michelson interferometer adversely. The resulting light scattering causes significant attenuation of intensity of the returning beam. Consequently, the maxima produced by interference between measurement and reference beams also suffer significant intensity losses. If the trigger input voltage decreases due to the intensity loss to the point that the trigger thresholds are no longer crossed, no further square-wave signals are produced and the counting operation is disabled. Thus the concentration of dust and vapor in the air determines the working range of this measurement technique.

In reduction of the wavelength the entire beam path between laser source and reference or measurement reflector is to be taken into account, since the laser beam is also subjected to the atmospheric influences between interferometer and the reference zero point of the measurement reflector.

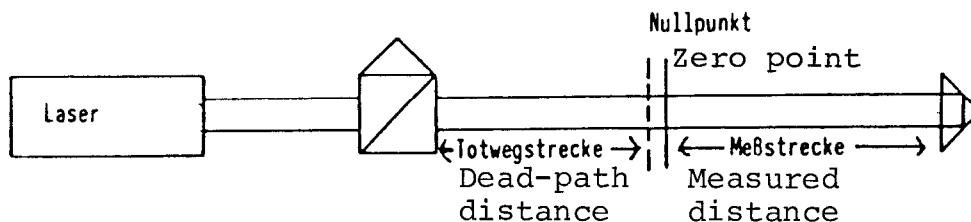


Figure 18

If this segment is disregarded in correcting the measurement values with the associated representative refractive index, the measurements will contain a dead-path error. This leads to a shift of the zero point if only the wavelength of the measured distance is corrected. The dead-path error can be prevented if additional temperature and pressure sensors are installed along the dead-path distance, in order to determine the atmospheric conditions existing there as well. These additional precautions are not needed if unnecessary dead-path distances are avoided. If the reference reflector is placed at a distance from the interferometer, a representative refractive index must be determined for the beam path as well.

3.3. Accuracy and resolution

The resolution of modern Michelson interferometers is around $\lambda/8$ (approximately 0.079 microns). The uncertainty in the value of the wavelength in vacuum of an Ne-He laser is smaller than 100 parts per billion. The frequency stability of the laser in vacuum ranges from 500 parts per billion to 100 parts per trillion. In order to determine the wavelength of the laser in air, it is necessary, as explained in Section 3.2.2, to know the dry-bulb temperature T , the wet-bulb temperature T' and the pressure of the air.

Our institute uses a "Hygrophyl Type 4455" psychrometer of the Ultrakust Company for measuring the dry-bulb and wet-bulb temperatures. With careful measurement, this instrument is capable of accuracy of $\pm 0.2^\circ\text{C}$. The air pressure can be determined with accuracy of ± 0.5 mbar by means of a mechanical barometer.

Substitution of these values in the equations derived for average atmospheric conditions

$$\begin{aligned}m_{nL}(T) &\sim \pm 8.5 \cdot 10^{-7} \cdot m_T \\m_{nL}(p) &\sim \pm 2.7 \cdot 10^{-7} \cdot m_p \\m_{nL}(T') &\sim \pm 1.5 \cdot 10^{-6} \cdot m_{T'}\end{aligned}$$

yields

$$m_{nL} (T) \sim \pm 1.70 \cdot 10^{-7}$$

$$m_{nL} (p) \sim \pm 1.34 \cdot 10^{-7}$$

$$m_{nL} (T') \sim \pm 3.07 \cdot 10^{-7}$$

and

$$m_{nL}^2 = (m_{nL} (T))^2 + (m_{nL} (p))^2 + (m_{nL} (T'))^2$$

$$m_{nL} = \pm 3.76 \cdot 10^{-7}$$

=====

To estimate the individual influences of the meteorological terms determined for the measured distance S, it is necessary to differentiate the equation

$$\lambda_L = \frac{\lambda_0}{n_L}$$

Thus

$$\frac{d\lambda_L}{dn_L} = -\frac{\lambda_0}{n_L^2} \quad \text{with} \quad \lambda_0 = \lambda_L \cdot n_L \quad \Rightarrow \quad \frac{d\lambda_L}{dn_L} = -\frac{\lambda_L}{n_L}$$

$$\text{with } \lambda_L \sim s \quad \Rightarrow \quad m_s^2 = \left(-\frac{s}{n_L}\right)^2 \cdot m_{nL}^2$$

$$m_s = \frac{s}{n_L} \cdot m_{nL}$$

$$\frac{m_s}{s} = \frac{m_{nL}}{n_L}$$

=====

The relative accuracy of the refractive index n_L is identical to the relative accuracy of the distance s .

Rearrangement yields:

$$\begin{aligned}
 m_s (T) &= \frac{m_{nL} (T)}{n_L} \cdot s && \sim \pm 1.70 \cdot 10^{-7} \cdot s \\
 m_s (p) &= \frac{m_{nL} (p)}{n_L} \cdot s && \sim \pm 1.34 \cdot 10^{-7} \cdot s \\
 m_s (T') &= \frac{m_{nL} (T')}{n_L} \cdot s && \sim \pm 3.07 \cdot 10^{-7} \cdot s
 \end{aligned}$$

Assuming that the errors are independent of each other, and introducing the errors in laser frequency, wavelength in vacuum and resolution, application of the error propagation theorem yields the following for m_s :

$$\begin{aligned}
 m_s^2 &= m_s (T)^2 + m_s (p)^2 + m_s (T')^2 + m_p^2 + m_\lambda^2 + m_\Delta^2 \\
 &= \frac{m_{nL} (T)^2}{n_L^2} \cdot s^2 + \frac{m_{nL} (p)^2}{n_L^2} \cdot s^2 + \frac{m_{nL} (T')^2}{n_L^2} \cdot s^2 + (5 \cdot 10^{-7} \cdot s)^2 + (1 \cdot 10^{-7} \cdot s)^2 \\
 &\quad + (0.079 \cdot 10^{-6} \mu m)^2 \\
 &= (m_{nL} (T)^2 + m_{nL} (p)^2 + m_{nL} (T')^2) \frac{s^2}{n_L^2} + (5 \cdot 10^{-7} \cdot s)^2 + (1 \cdot 10^{-7} \cdot s)^2 + (0.079 \cdot 10^{-6} \mu m)^2 \\
 &= m_{nL}^2 \cdot \frac{s^2}{n_L^2} + (5 \cdot 10^{-7} \cdot s)^2 + (1 \cdot 10^{-7} \cdot s)^2 + (0.079 \cdot 10^{-6} \mu m)^2 \\
 m_s &= \pm \sqrt{\left(\frac{s}{n_L} \right)^2 \cdot m_{nL}^2 + (5 \cdot 10^{-7} \cdot s)^2 + (1 \cdot 10^{-7} \cdot s)^2 + (0.079 \cdot 10^{-6} \mu m)^2}
 \end{aligned}$$

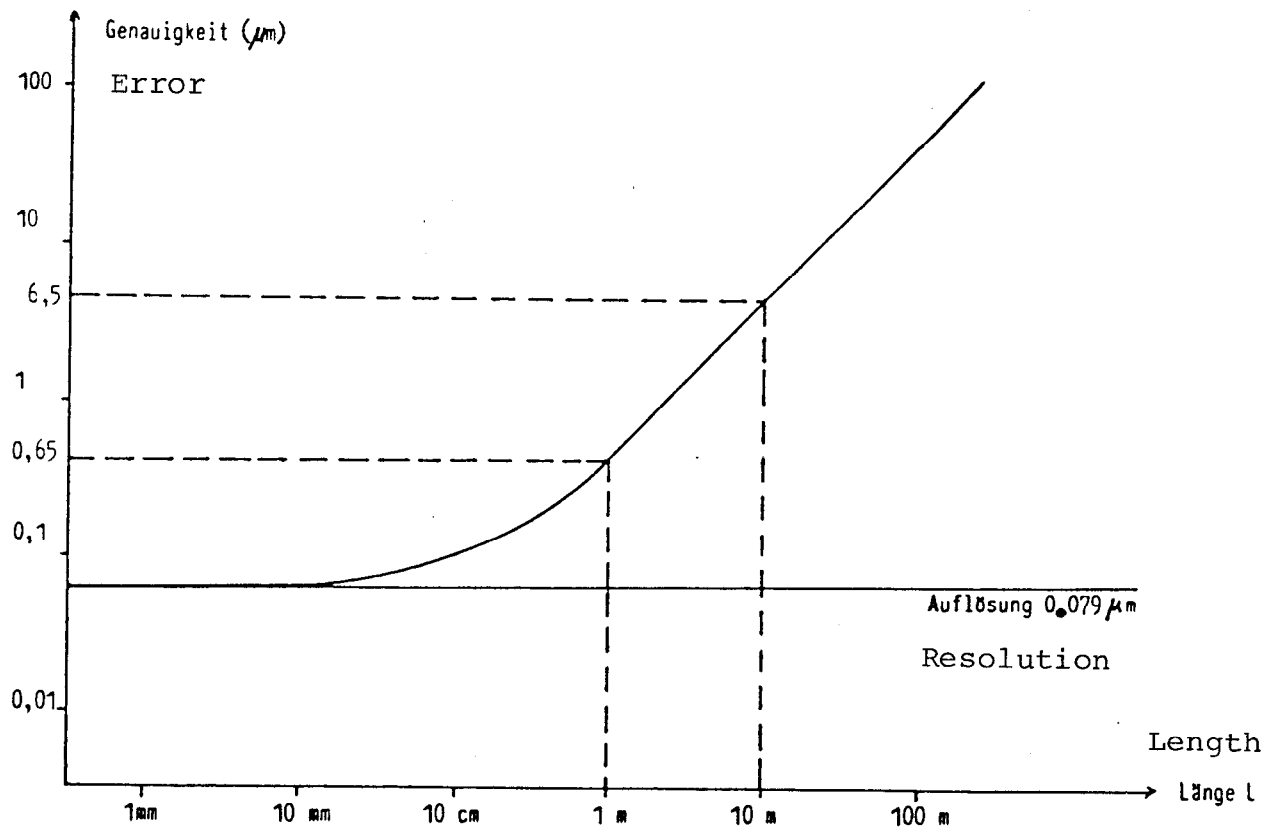


Figure 19

The mean distance error is plotted as a function of length in Figure 19. For lengths from 1 to 10 m, the error in distance measurement lies between 0.65 and 6.5 microns even without correcting for the influences of meteorology and frequency stability. Such accuracy is entirely adequate for calibration of geodetic instruments. For calibration of invar level rods, standard meters or stadia rods, a relative error of 1 micron per meter is usually expected in length

measurement. However, if lengths of several meters are to be measured with an accuracy on the order of 1/10 micron, it is absolutely necessary to correct for the influences of meteorology and frequency stability.

4. The laser Doppler interferometer

4.1. Mode of operation

A recent development is the laser Doppler interferometer of Hewlett-Packard. The measurement principle is very similar to that of the Michelson interferometer, but the Doppler effect produced by changing the beam path length is used instead of the number of interference maxima or minima for distance measurement. The layout of such an interferometer is shown in Figure 20. The light source is a helium-neon laser, tuned to emit only the red neon line ($\lambda = 0.6328$ microns) with high coherence. An axial magnetic field is applied to split the neon line by the Zeeman effect into two components of opposite circular polarization. The frequencies f_1 and f_2 of these components differ by 1.8 MHz. The average wavelength of the two components is used as the length standard. The two components are converted to orthogonal linear polarizations by means of a polarizing system consisting of a half-wave plate and a quarter-wave plate, and are then

expanded by a telescope. At the reference beam splitter a small fraction of both components is split off to provide laser control capability and to form the reference frequency. The main portion passes in a straight line through the reference beam splitter and continues to the interferometer. At the semitransparent mirror of the interferometer, the laser beam is again split, after which the two components are separated by polarizing filters F_1 and F_2 . Consequently, the fixed reflector is traversed by a light flux of frequency f_2 and the movable reflector is traversed by a light flux of frequency f_1 . If the external reflector is moved with velocity v , the value of f_1 , as already explained, is Doppler-shifted by $\pm f_D$ depending on the direction of motion. After traversing the cube-corner reflectors in the interferometer, the light beam with frequency f_2 and the measurement beam with frequency $f_1 \pm \Delta f$ are recombined in the interferometer. The reference-beam and measurement-beam components of orthogonal linear polarizations are directed to photodiodes, converted to electrical signals of the same frequency and superposed. Thus interference between the two components occurs only after they have been converted to electrical signals in the photodiode. Since the two components differ slightly in frequency, beating occurs as a result of interference between the components. The frequency of the reference signal is $f_1 - f_2$, and approximately 1.8 MHz; that of the measurement signal is $f_1 - f_2 \pm \Delta f$, and approximately 1.8 ± 1.55 MHz.

Prinzipeller Aufbau des Laser-Doppler-Interferometers

Schematic layout of the laser Doppler interferometer

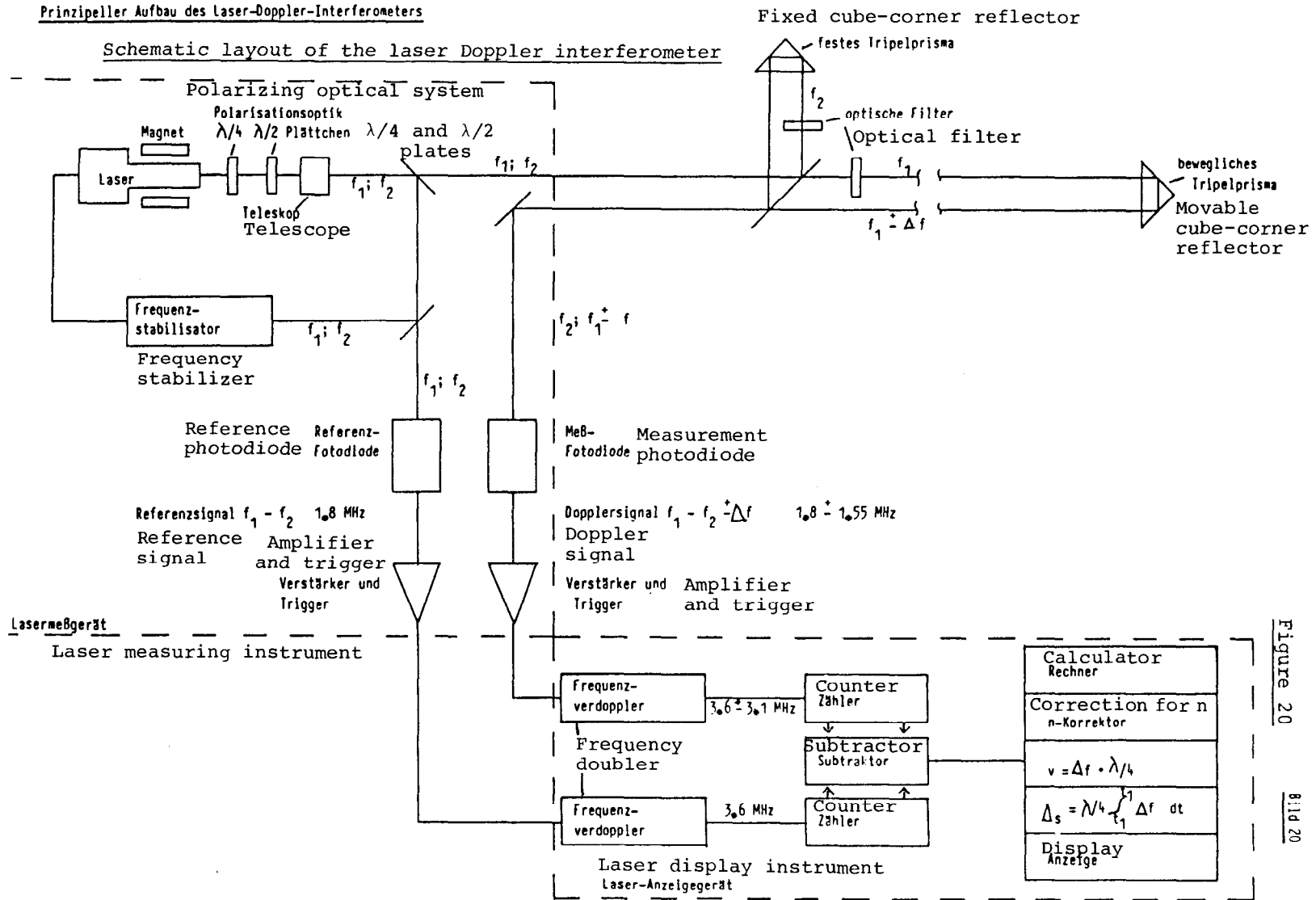


Figure 20

Bild 20

Figure 20

The signals then pass through an a.c. amplifier and are transformed to pulses in a trigger. Resolution is increased by doubling the frequency of both pulses. The pulses are counted in separate forward counters.

The subtractor continuously forms the difference Δf between the two counter totals. Because the pulse frequency is doubled, this difference is equal to $\pm 2 f_D$. The built-in calculator determines the velocity of motion of the reflector and the change in length of the measured distance at instants preprogrammed by the operator. A correction can be introduced for the change in wavelength as a function of the refractive index of the air. The velocity is calculated from the following formula:

$$v_p(t) = \pm \Delta f \cdot \frac{1}{n_L} \cdot \frac{\lambda_0}{4} \quad (\text{according to Doppler})$$

The unit of wavelength of the interferometer would actually have to be the wavelength λ_1 , since it was used for the distance measurement. However, the difference from the wavelength λ_0 is very small ($\pm 2 \times 10^{-9} \lambda_0$), and so λ_0 can be used in the calculation without loss of accuracy.

The individual velocities $v(t)$ are converted to lengths in the calculator by summing the individual amounts

$$\Delta f(t) \cdot \frac{\lambda_0}{4 \cdot n_L}$$

over the total measurement time. This corresponds to forming the time integral over the velocity:

$$\Delta_s = \frac{\lambda L}{4} \int_{z_1}^{z_2} \Delta f \, dt \quad *$$

4.2. Systematic errors of the laser Doppler interferometer

4.2.1. Effect of errors due to the laser

In principle, the lasers used for the laser Doppler interferometer are the same as those for the Michelson interferometer. The additional feature is the application of an axial magnetic field to the laser in order to split the neon line into two components. An examination of the laser for sources of systematic errors in distance measurement has already been discussed in Section 3.2.1.

In the Hewlett-Packard HP 5528A laser interferometer, which is available to our Institute, frequency stability is achieved by comparison of the intensities of the two components. These components are separated in the frequency stabilizer and their intensity difference is converted to error signals. These signals are sent to a piezoelectric element which is located in the beam tube and which continuously corrects the resonator length. Hewlett-Packard states that the minimum accuracy

* Translator's note: The lower limit of the integral was cut off in the original.

of the laser frequency with this type of frequency stabilization is better than 2 parts per billion.

4.2.2. Influence of refraction

Since the light wavelength is a measure of the optical path length travelled in the case of the laser Doppler interferometer as well, very accurate measurement of temperature and air pressure in the region of the measurement beam is again necessary to achieve highly accurate values of n_L and thus high distance-measuring accuracy. As explained in Section 3.2.2, the refractive index n_L can be determined with an accuracy of plus or minus 376 parts per billion by means of careful measurement of T , T' and p with the instruments used at our Institute.

A change of the phase relationship between measurement and reference beams, caused by air turbulences, has no effect on the interference of two waves with different frequencies. As is known from physics, the frequency is independent of atmospheric influences, and to this extent undisturbed frequency counting is possible. However, dust and vapor in the air can limit the working range even of this measurement technique. In addition, the influence of the atmosphere on the dead-path distance must also be taken into account in this technique.

The laser Doppler interferometer has the advantage that it is largely insensitive to atmospheric influences, and thus can be used even under fairly rough conditions. In contrast, the use of the Michelson interferometer is restricted to locales such as laboratories, which have homogeneous atmospheric conditions.

4.3. Accuracy and resolution

Because of a ten-fold improvement, the resolution of the laser Doppler interferometer is approximately 0.016 microns. The uncertainty in the value of the wavelength in vacuum of the He-Ne laser is smaller than 100 parts per billion. According to the manufacturer, the frequency stability is 2 parts per billion.

Using the instrumentation available at our Institute as described in Section 3.3, the refractive index of the air can be determined with a mean error of plus or minus 376 parts per billion.

Application of the error propagation theorem yields the following formula for the mean error of distance measurement:

$$m_s^2 = \left(\frac{s}{n_L}\right)^2 \cdot m_L^2 + m_f^2 + m_\lambda^2 + m_A^2$$

$$m_s = \pm \sqrt{\left(\frac{s}{n_L}\right)^2 \cdot m_L^2 + (2 \cdot 10^{-9} \cdot s)^2 + (1 \cdot 10^{-7} \cdot s)^2 + (0.016 \cdot 10^{-6} \text{ m})^2}$$

Figure 21 shows the mean error of the measured distance as a function of length. For lengths from 1 to 10 m, the error in distance measurement lies between 0.4 and 4.0 microns without correcting for meteorology and frequency stability. Comparison with the Michelson interferometer shows that the relative error in length measurement with the laser Doppler interferometer is 0.25 microns per meter more accurate. This improvement is due solely to the higher resolution and frequency stability of the laser Doppler interferometer.

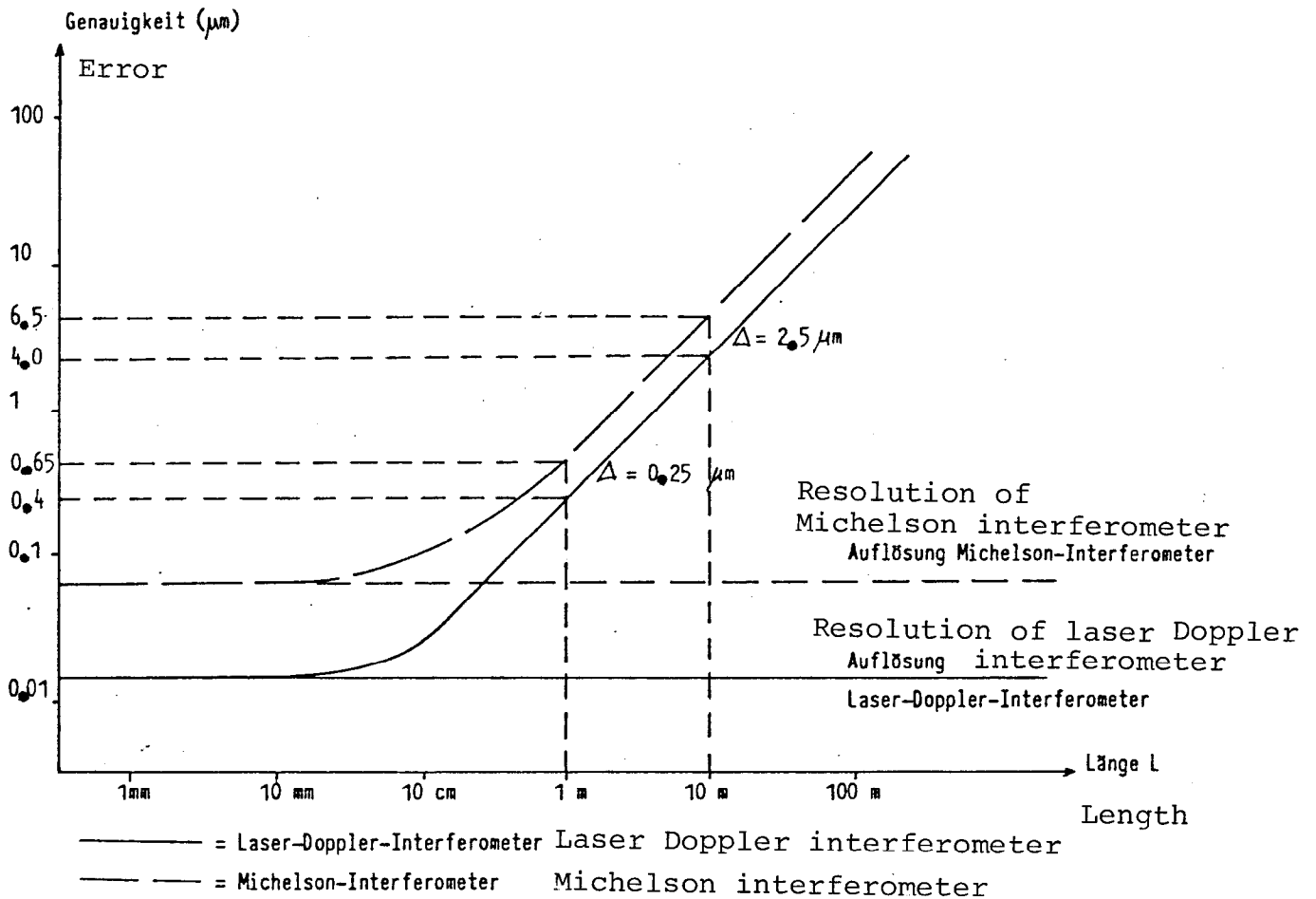


Figure 21

$$n_L = 1 + \frac{(n_{Ph} - 1)}{(1 + \alpha \cdot T)} \cdot \frac{p}{760} - \frac{0.055 \cdot 10^{-6}}{1 + \alpha \cdot T} \cdot 10^{\left(\frac{7.5 \cdot T'}{T' + 237.3} + 0.6609\right)} - 1/2 (T - T') \cdot \frac{p}{755}$$

for T in $^{\circ}C$, T' in $^{\circ}C$, p in Torr

$$n_L = 1 + \frac{(n_{Ph} - 1)}{(1 + \alpha \cdot T)} \cdot \frac{p}{1013.3} - \frac{4.125 \cdot 10^{-8}}{1 + \alpha \cdot T} \cdot 10^{\left(\frac{7.5 \cdot T'}{T' + 237.3} + 0.6609\right)} - 1/2 (T - T') \cdot \frac{p}{755}$$

for T in $^{\circ}C$, T' in $^{\circ}C$, p in mbar

$$n_L = 1 + \frac{(n_{Ph} - 1)}{(1 + \alpha \cdot T)} \cdot \frac{p}{1013.3} - \frac{0.055 \cdot 10^{-6}}{1 + \alpha \cdot T} \cdot 10^{\left(\frac{7.5 \cdot T'}{T' + 237.3} + 0.6609\right)} + \frac{4.125 \cdot 10^{-8} (T - T') \cdot p}{(1 + \alpha \cdot T) \cdot 2 \cdot 755}$$

$$n_L = 1 + \frac{(n_{Ph} - 1)}{(1 + \alpha \cdot T)} \cdot \frac{p}{1013.3} - \frac{0.055 \cdot 10^{-6}}{1 + \alpha \cdot T} \cdot 10^{\left(\frac{7.5 \cdot T'}{T' + 237.3} + 0.6609\right)} + \frac{4.125 \cdot 10^{-8} \cdot T \cdot p}{(1 + \alpha \cdot T) \cdot 1510} - \frac{4.125 \cdot 10^{-8} \cdot T' \cdot p}{(1 + \alpha \cdot T) \cdot 1510}$$

$$\frac{d_{nL}}{d_T} = -\alpha \frac{(n_{Ph} - 1) \cdot p}{(1 + \alpha \cdot T)^2 \cdot 1013.3} + \alpha \frac{0.055 \cdot 10^{-6}}{(1 + \alpha \cdot T)^2} \cdot 10^{\left(\frac{7.5 \cdot T'}{T' + 237.3} + 0.6609\right)} + \frac{p}{1510} \left(\frac{4.125 \cdot 10^{-8} (1 + \alpha \cdot T) - 4.125 \cdot 10^{-8} \cdot T \cdot \alpha}{(1 + \alpha \cdot T)^2} \right) + \alpha \frac{4.125 \cdot 10^{-8} \cdot T' \cdot p}{(1 + \alpha \cdot T)^2 \cdot 1510}$$

$$\frac{d_{nL}}{d_T} = -\alpha \frac{(n_{Ph} - 1) \cdot p}{(1 + \alpha \cdot T)^2 \cdot 1013.3} + \alpha \frac{0.055 \cdot 10^{-6}}{(1 + \alpha \cdot T)^2} \cdot 10^{\left(\frac{7.5 \cdot T'}{T' + 237.3} + 0.6609\right)} + \frac{4.125 \cdot 10^{-8} \cdot p}{(1 + \alpha \cdot T)^2 \cdot 1510} + \frac{4.125 \cdot 10^{-8} \cdot \alpha \cdot T' \cdot p}{(1 + \alpha \cdot T)^2 \cdot 1510}$$

$$\frac{d_{nL}}{d_p} = \frac{(n_{Ph} - 1)}{(1 + \alpha \cdot T) \cdot 1013.3} + \frac{4.125 \cdot 10^{-8} \cdot T}{(1 + \alpha \cdot T) \cdot 1510} - \frac{4.125 \cdot 10^{-8} \cdot T'}{(1 + \alpha \cdot T) \cdot 1510} = \frac{(n_{Ph} - 1)}{(1 + \alpha \cdot T) \cdot 1013.3} + \frac{4.125 \cdot 10^{-8}}{(1 + \alpha \cdot T) \cdot 1510} (T - T')$$

$$\frac{d_{nL}}{d_{T'}} = -\frac{0.055 \cdot 10^{-6}}{1 + \alpha \cdot T} \cdot 10^{\left(\frac{7.5 \cdot T'}{T' + 237.3} + 0.6609\right)} \cdot \ln 10 \cdot 10^{0.6609} - \frac{4.125 \cdot 10^{-8} \cdot p}{(1 + \alpha \cdot T) \cdot 1510}$$